Int. J. Solids Structures Vol. 30, No. 13, pp. 1807–1823, 1993
Printed in Great Britain

0020-7683/93 $6.00+.00

POWER LAW CREEP OF A COMPOSITE MATERIAL CONTAINING DISCONTINUOUS RIGID ALIGNED FIBERS

ROBERT M. MCMEEKING
Department of Materials and Department of Mechanical Engineering,
University of California, Santa Barbara, CA 93106, U.S.A.

(*Received* 16 *December* 1991; *in revised form* 24 *September* 1992)

Abstract—An asymptotic analysis is presented for the power law creep of a matrix containing discontinuous rigid aligned fibers. The fibers analysed have a high aspect ratio. As a result, the fiber length is much greater than both the fiber diameter and the spacing between neighboring fibers. For this situation, flow around the fiber ends can be neglected when the creep strength is being calculated. When the matrix is not slipping on the fiber surface or is nearly stuck, shearing flow dominates the behavior. The radial gradient of shear stress is balanced by the axial gradient of hydrostatic stress. Longitudinal, radial and circumferential deviatoric stresses are negligible. The resulting power law creep rate of the composite material is inversely proportional to the fiber aspect ratio raised to the power $1+1/n$ where n is the creep index. The fiber volume fraction also influences the creep rate. When the matrix slips freely on the fiber surface, or nearly so, stretching dominates the matrix flow. In this situation, the composite creep strength is not much better than the unreinforced matrix.

NOMENCLATURE

Note: superposed caret indicates a physical variable; a symbol without a caret is normalized and dimensionless, e.g. $\hat{a}$ is the fiber radius, a is $\hat{a}/\hat{b}$ where $\hat{b}$ is the unit cell radius.

$\hat{a}$	fiber radius
$\hat{b}$	unit cell radius
B	matrix creep rheology parameter
D	function of geometry and creep parameters; controls the creep strength
$\hat{e}$	axial strain rate
F	function for radial distribution of axial velocity
G	function controlling hydrostatic stress distribution
$\hat{L}$	fiber half length
m	interface drag exponent
n	matrix creep exponent
N	higher order term in creep strength
$\hat{r}$	radial coordinate
S	relative creep strength of composite material
$\tilde{S}$	scaled creep strength in excess of matrix strength
$\tilde{S}_k$	same as $\tilde{s}$ evaluated in Bao *et al.* (1991)
$\bar{S}$	average radial stress
$\underline{S}$	stress deviator
$\hat{v}$	velocity
V_f	fiber volume fraction
$\hat{z}$	axial coordinate
α	$\hat{L}/\hat{a}$ fiber aspect ratio
δ	$\hat{b}/\hat{L}$ small parameter
ε_e	effective strain rate
η	z/δ
λ	$\hat{L}/\hat{b}=1/\delta$
$\hat{\mu}$	interface drag parameter
ρ	integration variable
$\hat{\sigma}$	hydrostatic stress
$\underline{\hat{\sigma}}$	stress tensor
$\hat{\sigma}_a$	macroscopic axial stress
$\hat{\sigma}_f$	fiber axial stress
$\hat{\sigma}_m$	matrix axial stress
$\hat{\sigma}_e$	tensile equivalent stress
$\Sigma=(\hat{e}/B\delta)^{1/n}$	parameter for stress normalization
θ	circumferential coordinate.

INTRODUCTION

Cell models are popular and effective for estimating the creep strength of metal matrix fiber reinforced composites and such an approach has been used by Kelly and Street (1972), Dragone and Nix (1990), Goto and McLean (1991) and Bao *et al.* (1991b). For aligned discontinuous fibers, an individual reinforcement is considered embedded in a unit cell of the matrix material such that the volume ratio of fiber to matrix in the unit cell equals the average ratio in the composite material. Boundary conditions to cause the deformation are imposed on the perimeter of the unit cell to enforce periodicity and symmetry. For the creep response to tensile stresses aligned with the axis of circular fibers, it is sufficient to calculate the behavior of an axisymmetric cell such as that shown in Fig. 1. The deformation imposed on the cell forces it to retain its circular cylindrical shape. Each point on the surface of the cell is free of shear traction. The average transverse stress on the cell is zero and appropriate conditions are imposed at the interface between the fiber and the matrix material. In the annotations in Fig. 1 the conditions appropriate to an interface around a rigid fiber without debonds but with a nonlinear viscous sliding behavior are stated. In general, however, any physical assumption can be incorporated into the cell model such as fiber elasticity or creep, debonding of the interface, etc.

Cell models usually require a numerical treatment as undertaken by Dragone and Nix (1990) and Bao *et al.* (1991b). However, in certain circumstances an approximate model is accurate and can be analysed without recourse to complete numerical treatment. This approach has been used by Kelly and Street (1972) and Goto and McLean (1991). One such circumstance is when the fibers are aligned and have an aspect ratio which is high and a volume fraction that is moderate to high. Then the matrix segment around the fiber (with section ABCD in Fig. 1) is slender and can be readily analysed with approximate flow fields. In addition, the flow in the remaining matrix segment at the fiber ends does not need to be analysed accurately because it contributes little to the yield or creep strength compared to the matrix around the fiber. That is, when the fiber aspect ratio is high, the energy dissipation in the fiber end regions during matrix creep is negligible compared to the energy dissipation rate in the matrix surrounding the fiber. The creep strength is directly related to the energy dissipation rate, so it can be analysed by calculating the major contributions to the energy dissipation rate. In this paper, that is achieved by analysing the creeping flow of the matrix adjacent to the fiber sides. If this approach is unsatisfactory in a particular case, it can always be rectified by considering longer fibers, thereby making the fiber end regions relatively less important. In this sense, the analysis can always be justified by taking

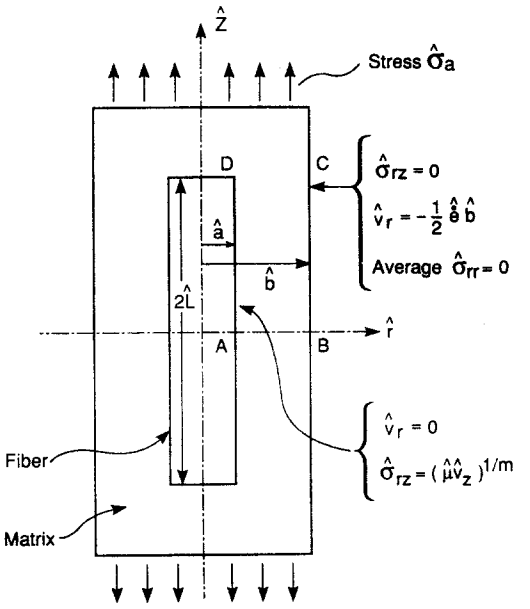

Fig. 1. Unit cell for matrix creep analysis.

the asymptotic limit of extremely long fibers. However, the analysis is proposed as being justifiable for fibers with a range of finite aspect ratios.

The issue has been studied by Bao *et al.* (1991a) for layered composites with perfectly plastic matrices. Bao *et al.* found that less than 10% of the yield strength is due to the end region when the volume fraction of rigid reinforcements is 25% and their aspect ratio is 100. For smaller aspect ratios the contribution from the end region is a higher fraction but can be modeled in an ad hoc manner as was demonstrated by Bao *et al.* (1991a). In addition, the aspect ratio of the cell relative to the aspect ratio of the fiber is known to affect the prediction of strength significantly which was demonstrated by Bao *et al.* (1991b). Thus, it is likely that the choice of aspect ratio of the cell will also influence how much of the strength is due to the matrix material around the fiber compared to the amount due to the material at the fiber ends. For example, choosing the aspect ratio of the cell to be the same as the aspect ratio of the fiber, as Bao *et al.* (1991a) did, is likely to exaggerate the importance of the fiber end region for high aspect ratio cases. A perhaps more sensible choice, in which the distance between the fiber and the cell edge is the same at the end and on the side, is likely to diminish the importance of the matrix at the fiber ends and so the 10% contribution mentioned above is probably an overestimate. At the other extreme of the rheology, namely a linearly viscous matrix, an argument can be made that as well as fiber end regions occupying relatively small volumes of the total composite microstructure, any non-uniformity of flow which they induce will be confined to the fiber end region by a St Venant effect. Thus, for all types of matrix an analysis concerned only with the matrix material surrounding the fibers circumferentially can be justified in certain cases.

In particular, the problem of a high aspect ratio rigid fiber embedded in a power law creeping matrix can be analysed in terms of the matrix material around the fiber. The cell shown in Fig. 1 will be used. The fiber is bonded to the matrix so that the radial velocity at the fiber is zero. However, it is assumed that the bond, or thin layer of interphase material at the interface, has a power law rheology of its own which allows slip of the matrix relative to the fiber. The end of the fiber is bonded strongly to the matrix as well, so that matrix incompressibility forces a net matrix flow parallel to the fiber. The axisymmetric quasistatic creeping response to an axial stress is considered. A power law rheology is assumed so that the analysis represents the steady state creep of metal or ceramic matrices around rigid (e.g. ceramic) fibers.

PROBLEM FORMULATION

The domain of the problem is the axisymmetric region with section ABCD in Fig. 1 ($\hat{a} \leqslant \hat{r} \leqslant \hat{b}$; $0 \leqslant \hat{z} \leqslant \hat{L}$). In cylindrical polar coordinates, the governing equilibrium equations neglecting inertia and body forces are

$$\frac{\partial \sigma_{rr}}{\partial r} + \frac{\sigma_{rr} - \sigma_{\theta\theta}}{r} + \delta \frac{\partial \sigma_{rz}}{\partial z} = 0, \tag{1}$$

$$\frac{\partial \sigma_{rz}}{\partial r} + \frac{\sigma_{rz}}{r} + \delta \frac{\partial \sigma_{zz}}{\partial z} = 0, \tag{2}$$

where $\boldsymbol{\sigma}$ is a scaled stress such that

$$\hat{\boldsymbol{\sigma}} = \Sigma \boldsymbol{\sigma}, \tag{3}$$

with $\hat{\boldsymbol{\sigma}}$ being the Cauchy stress and Σ a scaling parameter to be discussed later. The components r and z are scaled measures of position defined by

$$\hat{r} = \hat{b} r \tag{4}$$

and

$$\hat{z} = \hat{L}z, \tag{5}$$

where $\hat{r}$, $\hat{z}$, $\hat{b}$ and $\hat{L}$ are specified in Fig. 1. The parameter δ is such that

$$\delta = \hat{b}/\hat{L}, \tag{6}$$

and in the problems to be analysed is much less than 1. The choice of differential scaling for r and z introduces a coordinate stretching transformation (Van Dyke, 1975) which will be useful in the subsequent analysis.

The matrix creeps with a power law incompressible rheology given by

$$\hat{e}_{ij} = \tfrac{3}{2}B\hat{\sigma}_e^{n-1}\hat{S}_{ij}, \tag{7}$$

where $\hat{\mathbf{e}}$ is the strain rate, $\hat{\mathbf{S}}$ is the deviatoric stress given by

$$\hat{S}_{ij} = \hat{\sigma}_{ij} - \hat{\sigma}\delta_{ij}, \tag{8}$$

where $\hat{\sigma}(=\hat{\sigma}_{kk}/3)$ is the hydrostatic part of the stress, $\hat{\sigma}_e$ is the effective stress such that

$$\hat{\sigma}_e = \sqrt{\tfrac{3}{2}\hat{S}_{ij}\hat{S}_{ij}}, \tag{9}$$

and B is a material constant which is, however, dependent on temperature. Note that in uniaxial stress the axial strain rate equals B times the nth power of the stress. In terms of scaled variables, the creep law can be written as

$$\frac{\partial v_r}{\partial r} = \tfrac{3}{2}\sigma_e^{n-1}S_{rr}, \tag{10}$$

$$\frac{v_r}{r} = \tfrac{3}{2}\sigma_e^{n-1}S_{\theta\theta}, \tag{11}$$

$$\delta\frac{\partial v_z}{\partial z} = \tfrac{3}{2}\sigma_e^{n-1}S_{zz}, \tag{12}$$

$$\frac{\partial v_z}{\partial r} + \delta\frac{\partial v_r}{\partial z} = 3\sigma_e^{n-1}\sigma_{rz}, \tag{13}$$

where $\hat{\mathbf{v}}$ is the velocity and

$$\hat{\mathbf{v}} = \hat{b}B\hat{\Sigma}^n\mathbf{v}. \tag{14}$$

On AB ($z = 0$) the boundary conditions by symmetry are

$$v_z(r, 0) = 0, \tag{15}$$

$$\sigma_{rz}(r, 0) = 0. \tag{16}$$

On AD ($r = a = \hat{a}/\hat{b}$) one boundary condition is

$$v_r(a, z) = 0, \tag{17}$$

while the slip condition (see Fig. 1) becomes

$$v_z(a, z) = \sigma_{rz}^m/\mu, \tag{18}$$

where

$$\mu = \hat{\mu} B \hat{b} \Sigma^{n-m}, \tag{19}$$

and $\hat{\mu}$ is a slip parameter for the interface. It should be noted that the last boundary condition can represent a variety of physical situations. One possibility is that there is a thin but distinct interphase of thickness $\hat{t}$ so that $V_z(a, z)/\hat{t}$ is the shear strain rate in the interphase. Equation (18) then implies that the interphase is subject to power law creep but with an exponent m and the coefficient in the creep law is $1/(3^{(m+1)/2}\hat{\mu}\hat{t})$ replacing B in eqn (7). Another possibility is that there is no interphase but instead the fiber has a rough surface over which the matrix must flow even though the bond between the matrix and the fiber is relatively weak in shear. In that case, the index m would equal n and the slip parameter $\hat{\mu}$ would depend on the roughness of the fiber surface which would provide drag.

On BC ($r = 1$) the boundary conditions are

$$\sigma_{rz}(1, z) = 0 \tag{20}$$

and

$$v_r(1, z) = -\tfrac{1}{2}\delta, \tag{21}$$

where

$$\hat{e} = B\Sigma^n \delta \tag{22}$$

is the axial strain rate. The condition in eqn (21) means that the scaled axial strain rate is equal to δ. This choice is arbitrary, though convenient. As a consequence, eqn (22) establishes Σ in terms of $\hat{e}$, the axial strain rate in physical variables. The boundary condition, eqn (21), states that the unit cell remains a cylinder of uniform diameter. As a result, the normal stress σ_{rr} is not uniformly zero on $r = 1$. However, the average of σ_{rr} on $r = 1$ can be set to zero so that

$$\int_0^1 \sigma_{rr}(1, z)\, dz = 0 \tag{23}$$

to ensure that the transverse stress is approximately zero. The approximation arises because the cell extends a small distance above C, but that portion is neglected. The boundary condition equation (23), can be met through adjustment of the hydrostatic stress.

Note that no explicit boundary conditions are posed for CD. The average stress there will be of interest and determines $\hat{\sigma}_a$. The creep strength S of the composite material is defined as the average axial stress in the composite at a given axial strain rate divided by the stress in the matrix alone at the same axial strain rate. That is

$$S = \hat{\sigma}_a(\hat{e})/(\hat{e}/B)^{1/n}, \tag{24}$$

where $\hat{\sigma}_a$ is a function of the axial strain rate $\hat{e}$.

ASYMPTOTIC ANALYSIS

A perturbation series solution will be developed. It will have much in common with the outer solution for a plane strain power law squeeze film due to Johnson (1984). In addition, there are boundary layers, but fully matched solutions will not be established in them. In the outer solution for the fiber problem, the matrix flow is dominated by shearing and the shear stress can be expanded in integer powers of δ, so that

$$\sigma_{rz} = \sigma_{rz}^{(0)} + \delta\sigma_{rz}^{(1)} + O(\delta^2). \tag{25}$$

As a consequence of eqn (13), v_z is $O(1)$ at leading order so

$$v_z = v_z^{(0)} + \delta v_z^{(1)} + O(\delta^2). \tag{26}$$

Incompressibility [i.e. the sum of eqns (10)–(12)] then implies that

$$v_r = \delta v_r^{(1)} + O(\delta^2), \tag{27}$$

and, apart from σ_{rz}, S_{ij} is $O(\delta)$, so

$$S_{rr} = \delta S_{rr}^{(1)} + O(\delta^2), \tag{28}$$

etc. Any gradient of σ_{rz} in the r direction must be balanced by a gradient of σ_{zz} in the z direction. For this to be possible, the stress σ_{zz} must be $O(1/\delta)$ so that the contribution of the longitudinal gradient of σ_{zz} to eqn (2) is $O(1)$ which is the same order of magnitude as the contribution of the shear stress gradient in eqn (2). This suggests

$$\sigma = \frac{1}{\delta}\sigma^{(-1)} + \sigma^{(0)} + O(\delta) \tag{29}$$

so that the hydrostatic stress is an order of magnitude larger than the deviatoric stress.

The leading order governing equations can now be stated. With terms of higher order omitted, it is found that eqn (1) gives

$$\frac{\partial \sigma^{(-1)}}{\partial r} = 0, \tag{30}$$

while eqn (2) provides

$$\frac{\partial \sigma_{rz}^{(0)}}{\partial r} + \frac{\sigma_{rz}^{(0)}}{r} + \frac{\partial \sigma^{(-1)}}{\partial z} = 0. \tag{31}$$

The creep relationship of eqn (13) gives

$$\frac{\partial v_z^{(0)}}{\partial r} = 3(\sigma_e^{(0)})^{n-1}\sigma_{rz}^{(0)}, \tag{32}$$

where

$$\sigma_e^{(0)} = \sqrt{3}\,|\sigma_{rz}^{(0)}|, \tag{33}$$

while incompressibility provides

$$\frac{\partial v_r^{(1)}}{\partial r} + \frac{v_r^{(1)}}{r} + \frac{\partial v_z^{(0)}}{\partial z} = 0. \tag{34}$$

Equations (15)–(23) give the boundary conditions

$$v_z^{(0)}(r, 0) = 0, \tag{35}$$

$$\sigma_{rz}^{(0)}(r, 0) = 0, \tag{36}$$

$$v_r^{(1)}(a, z) = 0, \tag{37}$$

$$v_z^{(0)}(a,z) = (\sigma_{rz}^{(0)})^m/\mu, \tag{38}$$

$$v_r^{(1)}(1,z) = -\tfrac{1}{2}, \tag{39}$$

$$\sigma_{rz}^{(0)}(1,z) = 0 \tag{40}$$

and

$$\int_0^1 \sigma^{(-1)}(1,z)\,\mathrm{d}z = 0. \tag{41}$$

Solution

Equation (30) shows that $\sigma^{(-1)}$ is independent of r. Therefore, integration of eqn (31) subject to eqn (40) gives

$$\sigma_{rz}^{(0)} = \frac{1}{2}\left(\frac{1}{r} - r\right)\frac{\mathrm{d}\sigma^{(-1)}}{\mathrm{d}z}. \tag{42}$$

It will be confirmed that $\mathrm{d}\sigma^{(-1)}/\mathrm{d}z$ is positive for $z > 0$ and thus so is $\sigma_{rz}^{(0)}$. Consequently eqn (32) shows that

$$\frac{\partial v_z^{(0)}}{\partial r} = \frac{3^{(n+1)/2}}{2^n}\left(\frac{1}{r} - r\right)^n\left(\frac{\mathrm{d}\sigma^{(-1)}}{\mathrm{d}z}\right)^n. \tag{43}$$

Integration of eqn (42) with eqn (37) provides

$$v_z^{(0)} = \frac{1}{\mu 2^m}\left(\frac{1}{a} - a\right)^m\left(\frac{\mathrm{d}\sigma^{(-1)}}{\mathrm{d}z}\right)^m + F(r,a,n)\left(\frac{\mathrm{d}\sigma^{(-1)}}{\mathrm{d}z}\right)^n, \tag{44}$$

where

$$F(r,a,n) = \frac{3^{(n+1)/2}}{2^n}\int_a^r \left(\frac{1}{\rho} - \rho\right)^n \mathrm{d}\rho. \tag{45}$$

Differentiation of eqn (44) with respect to z provides the axial strain rate which is inserted into eqn (34). Integration of eqn (34) with respect to r combined with boundary condition equation (37) then gives

$$v_r^{(1)} = \frac{1}{\mu 2^{m+1}}\left(\frac{1}{a} - a\right)^m\left(\frac{a^2}{r} - r\right)\frac{\mathrm{d}}{\mathrm{d}z}\left(\frac{\mathrm{d}\sigma^{(-1)}}{\mathrm{d}z}\right)^m - \frac{1}{r}\int_a^r \rho F(\rho,a,n)\,\mathrm{d}\rho\,\frac{\mathrm{d}}{\mathrm{d}z}\left(\frac{\mathrm{d}\sigma^{(-1)}}{\mathrm{d}z}\right)^n. \tag{46}$$

The boundary condition specifying the strain rate, eqn (38), then provides the nonlinear differential equation

$$\frac{\mathrm{d}}{\mathrm{d}z}\left[G(a,n)\left(\frac{\mathrm{d}\sigma^{(-1)}}{\mathrm{d}z}\right)^n + \frac{(1-a^2)^{m+1}}{\mu 2^{m+1}a^m}\left(\frac{\mathrm{d}\sigma^{(-1)}}{\mathrm{d}z}\right)^m\right] = \frac{1}{2}, \tag{47}$$

where

$$G(a,n) = \int_a^1 \rho F(\rho, a, n)\, \mathrm{d}\rho. \tag{48}$$

This can be integrated once and boundary condition equation (36) along with eqn (42) can be used to give

$$G(a,n)\left(\frac{\mathrm{d}\sigma^{(-1)}}{\mathrm{d}z}\right)^n + \frac{(1-a^2)^{m+1}}{\mu 2^{m+1} a^m}\left(\frac{\mathrm{d}\sigma^{(-1)}}{\mathrm{d}z}\right)^m = \frac{z}{2}. \tag{49}$$

This is hard to solve in general when $m \neq n$ except when $n = 2$ and $m = 1$ and vice versa. Substantial insight and a degree of generality can be retained by choosing $m = n$. As discussed previously, this case represents that of a well bonded fiber–matrix interface with a rough fiber surface at a temperature sufficiently high to give rise to a negligible shear strength of the bonded interface. The resistance to slip arises from the drag induced by the creep of the matrix along the rough fiber suface. Alternately, it could represent the case of an interphase with the same creep index as the matrix but with a different creep coefficient. The approach of using $m = n$ permits the study of the effect of a weak interface and some general insights are obtained. With $m = n$, eqn (49) provides

$$\frac{\mathrm{d}\sigma^{(-1)}}{\mathrm{d}z} = \left(\frac{z}{D}\right)^{1/n}, \tag{50}$$

where

$$D(a,n) = 2G(a,n) + \frac{(1-a^2)^{n+1}}{\mu 2^n a^n}. \tag{51}$$

Integration of eqn (49) and use of eqn (41) reveals that

$$\sigma^{(-1)} = \frac{z^{1+1/n} - \dfrac{n}{2n+1}}{\left(1+\dfrac{1}{n}\right)D^{1/n}}. \tag{52}$$

The remaining significant terms in the solution are then

$$\sigma_{rz}^{(0)} = \frac{1}{2}\left(\frac{1}{r} - r\right)\left(\frac{z}{D}\right)^{1/n}, \tag{53}$$

$$v_z^{(0)} = \left[\frac{1}{\mu 2^n}\left(\frac{1}{a} - a\right)^n + F(r,a,n)\right]\frac{z}{D}, \tag{54}$$

$$v_r^{(1)} = -\left[\frac{1}{\mu 2^{n+1}}\left(\frac{1}{a} - a\right)^n\left(r - \frac{a^2}{r}\right) + \frac{1}{r}\int_a^r \rho F(\rho, a, n)\, \mathrm{d}\rho\right]\frac{1}{D}. \tag{55}$$

Thus the key assumption made by Kelly and Street (1972) that the velocity in the z direction is proportional to z is correct to leading order. However, now the dependence on r has been established too.

Boundary layer

It is possible to proceed with the solution to higher order terms and so establish the small corrections involved but this will not be done here. However, it should be noted that boundary layers are involved at $z = 0$ and at $r = 1$. The shear stress to leading order is zero

at those locations and thus so is the effective stress σ_e. In the pure power law rheology being used in this problem, this makes the matrix rigid to leading order at $z = 0$ and $r = 1$. However, material is deforming at those locations and as a result the higher order terms in the deviatoric stress in the perturbation series diverge there. To correct this, a boundary layer analysis is required. However, the result of Johnson (1984) for the plane strain squeeze film indicates that the boundary layers are passive and so do not disrupt the leading order outer solution. Consequently, the leading order outer solution equations (52)–(55) are valid. The boundary layer analysis provides a significant correction term at higher order in the outer solution. This correction term has not been worked out. However, the boundary layer at $z = 0$ can be analysed and terms for the correction estimated there. An overall axial balance of stress then provides the net resultant stress for the composite material and therefore an estimate to higher order of the creep strength of the composite. The details of the boundary layer results are developed in the Appendix.

COMPOSITE MATERIAL CREEP RESPONSE

We now have an estimate for the average axial stress at $z = 1$ in the cell. This is given by eqn (52) at $z = 1$ divided by δ plus the correction $\delta^{1/n}N$ arising from the analysis of the boundary layer at $z = 0$ [see eqns (A16), (A22) and (A28)]. The correction is required at $z = 1$ to balance the tension in the boundary layer at $z = 0$. Thus, the average stress at $z = 1$ in normalized variables is

$$\frac{n}{\delta(2n+1)D^{1/n}} + \delta^{1/n}N. \tag{56}$$

Clearly, as long as D is not large, the first term will be the largest contribution to $\hat{\sigma}_a$ (see Fig. 1) which represents the creep stress of the composite material. Additional contributions to $\hat{\sigma}_a$ will arise from the effects of matrix flow around the fiber end. This term may be of the same order of magnitude as the boundary layer term N, but the fiber end flow term is difficult to estimate. Although it may be inconsistent, we will simply omit the fiber end flow term but include the boundary term. It is hoped that the result will then be meaningful for low fiber volume fractions where the fiber end flow term will tend to be small. In any case, as long as D is not large, the discrepancy relates only to a higher order term and the creep behavior predicted by the leading order term in eqn (56) is still reliable. The omission will be more serious in the case of low drag fiber–matrix interfaces with moderate to high volume fractions of fibers because D becomes large in that case. Then the fiber end term will be just as significant as the leading term in eqn (56). The validity of the model is then doubtful.

The estimate for $\hat{\sigma}_a$ is obtained from eqn (56) in physical variables. Accordingly

$$\begin{aligned}\hat{\sigma}_a &= \frac{\Sigma \hat{L} n}{\hat{b}(2n+1)D^{1/n}} + \Sigma N \delta^{1/n} \\ &= \left(\frac{\hat{\dot{e}}}{B}\right)^{1/n}\left[\frac{\lambda^{1+1/n}n}{(2n+1)D^{1/n}} + N\right],\end{aligned} \tag{57}$$

where $\lambda = \hat{L}/\hat{b}$. In turn, the creep strength is

$$S = \frac{\lambda^{1+1/n}n}{(2n+1)D^{1/n}} + N. \tag{58}$$

Note that the term S functions as a dimensionless reference stress (Leckie, 1986) for the creep behavior of the composite as in

$$\hat{e} = B(\hat{\sigma}_a/S)^n. \tag{59}$$

The results will be left in the form presented in eqns (57) and (58) even though the dependence on parameters like fiber volume fraction and fiber aspect ratio is not apparent. The forms presented, in terms of a and λ, are more versatile with the advantage that there is no asumption dependent conversion from a and λ to volume fraction and fiber aspect ratio. However, such conversions can be made easily by the user of the results. For example, Kelly and Street (1972) neglected the ends of the unit cell and assumed that $\hat{b}$ is half the nearest neighbor center to center spacing in a hexagonal array of fibers. In that case

$$a = \hat{a}/\hat{b} = (2\sqrt{3}\,V_f/\pi)^{1/2}, \tag{60}$$

where V_f is the fiber volume fraction. On the other hand, if the unit cell is assumed to have the same aspect ratio as the fiber, then

$$a = V_f^{1/3}. \tag{61}$$

Therefore, it is best to avoid any conversion and leave the user of the results to choose an approach which is appropriate to the material of interest.

In any case, since

$$\lambda = \hat{L}/\hat{b} = (\hat{L}/\hat{a})(\hat{a}/\hat{b}) \tag{62}$$

λ will be proportional to the aspect ratio of the fiber $\alpha = \hat{L}/\hat{a}$. Therefore, the creep strength S, eqn (58), depends relatively strongly on the fiber aspect ratio, being proportional to $\alpha^{1+1/n}$. This ranges from a quadratic dependence for linear viscosity to nearly linear for high n. This dependence was identified by Kelly and Street (1972). As the fiber volume fraction increases, a will increase and be around unity for fiber volume fractions around unity. This will cause D to become very small or zero, predicting very large or infinite creep strengths. This locking up is present in the model of Kelly and Street (1972), occurring at $V_f = 0.91$ in that case, which is when fibers in a hexagonal array touch each other.

As the fiber volume fraction approaches zero with μ finite, a will disappear and so will the creep strength predicted by the first term in eqn (58). The second term, N, then provides the creep strength, which will be unity according to eqn (A22). Returning to the general case, consider what happens if $\mu \to 0$. This is the zero drag case and eqn (51) makes it clear that $D \to \infty$. Consequently, the creep strength is then given by N, expressed in this case by eqn (A28). Results for N for several values of n are plotted in Fig. 2. The values are less

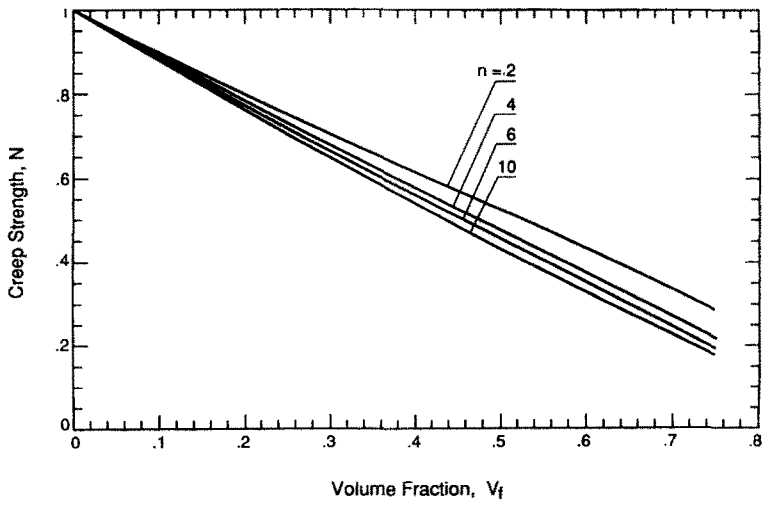

Fig. 2. Creep strength of a material with zero drag between the fiber and the matrix.

than or equal to unity, indicating that the composite will be weaker than the matrix alone. This effect occurs because the fibers act only to fill cylindrical holes in the matrix and the composite behavior represents the creep of a matrix filled with such cylindrical holes. It can be seen in Fig. 2 that N is approximately given by $1-V_f$, confirming this effect. This result is not exact because the effect of flow around the fiber end has been neglected. The true result is probably $1-V_f$ plus a small amount accounting for the fiber end effect. However, the magnitude of the contribution due to flow around the very end of the fiber will not depend to any great extent on the aspect ratio of the fiber. Thus, for long, discontinuous fibers, the creep strength will be modest if the matrix is free to slip without drag relative to the fiber. This effect was apparent, although not emphasized, in the model of Kelly and Street (1972).

It is difficult to know realistic physical values of μ. In addition, the model for interface drag with $m = n$ is of limited value although it is very similar to a form implied in the model of Kelly and Street (1972). As they pointed out (in terms of their interface sliding parameter but the implications are the same), a given value of μ (less than ∞) will have a stronger effect on the creep strength of a material with a low n compared to a high n. This arises because S is controlled by $D^{-1/n}$ and μ enters the creep strength to leading order through D. However, the effect of a more physically realistic slip law remains to be investigated. For example, interface diffusion tends to occur readily in metal matrix composites at creep temperatures. This will tend to induce slipping with a linear rheology, i.e. $m = 1$ in eqn (18).

Finally, we can consider the creep strength in detail for the no slip case $\mu = \infty$. This is accomplished by consideration of $\tilde{S} = (S-1)/\alpha^{1+1/n}$ computed from eqn (58). This parameter is the excess creep strength over the matrix strength normalized to make it independent of α. The result is plotted as a function of a^2 in Fig. 3 for several creep exponents. For comparison, the equivalent parameter from the model of Kelly and Street (1972) is plotted as well. For the latter model, the volume fraction has been converted to a by use of eqn (60). The result has the form

$$\tilde{S}_K = (S-1)/\alpha^{1+1/n} = \left(\frac{2}{3}\right)^{1/n} \frac{n}{2n+1} \left(\frac{a}{1-a}\right)^{1/n} \frac{a^2}{1-a^2}. \tag{63}$$

It can be seen in Fig. 3 that there are significant differences between the two models.

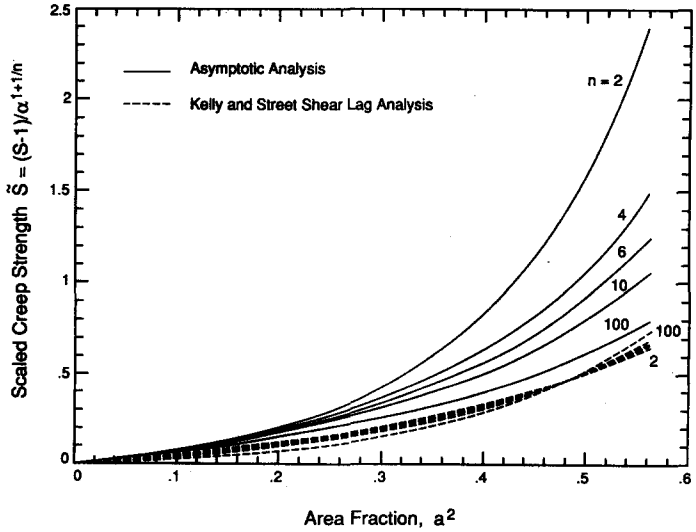

Fig. 3. Excess creep strength of a material with no slip between the fiber and the matrix. The result is normalized by the fiber aspect ratio raised to the power $1+1/n$.

FIBER STRESSES

Fiber stresses are important because the reinforcements can crack and degrade the creep strength when the stress exceeds the fiber strength as observed by Weber *et al.* (1993). In addition, Sancaktar and Zhang (1990) have demonstrated that high shear stresses on the interface can cause interphase and matrix cracking. The shear stress at the interface between the matrix and the fiber is directly related to the gradient of the average axial fiber stress along the fiber. The average axial stress at any point in the fiber can be computed from a net balance of forces in the axial direction. This requires

$$\hat{\sigma}_a = a^2\hat{\sigma}_f(\hat{z}) + (1-a^2)\hat{\sigma}_m(\hat{z}) \tag{64}$$

at any position $\hat{z}$ where $\hat{\sigma}_f$ is the average axial fiber stress at $\hat{z}$ and $\hat{\sigma}_m$ is the average axial matrix stress at $\hat{z}$. From eqn (52) we have

$$\hat{\sigma}_m(\hat{z}) = \left(\frac{\hat{e}}{B}\right)^{1/n}\left\{\frac{\left[\left(\frac{\hat{z}}{\hat{L}}\right)^{1+1/n} - \frac{n}{2n+1}\right]\lambda^{1+1/n}}{(1+1/n)D^{1/n}} + N\right\}. \tag{65}$$

Given eqn (57), it follows that

$$\hat{\sigma}_f(\hat{z}) = \left(\frac{\hat{e}}{B}\right)^{1/n}\left\{\frac{\lambda^{1+1/n}}{D^{1/n}}\frac{n}{n+1}\left[\frac{1}{a^2} - \frac{1-a^2}{a^2}\left(\frac{\hat{z}}{\hat{L}}\right)^{1+1/n} - \frac{n}{2n+1}\right] + N\right\}. \tag{66}$$

The highest value is at $\hat{z} = 0$ where

$$\begin{aligned}\hat{\sigma}_f^{\max} &= \hat{\sigma}_f(0)\\ &= \left(\frac{\hat{e}}{B}\right)^{1/n}\left[\frac{\lambda^{1+1/n}}{D^{1/n}}\frac{n}{n+1}\left(\frac{1}{a^2} - \frac{n}{2n+1}\right) + N\right].\end{aligned} \tag{67}$$

Neglecting N, which will be small compared to other terms when λ is large, we find

$$\frac{\hat{\sigma}_f^{\max}}{\hat{\sigma}_a} = \frac{2n+1-a^2n}{a^2(n+1)}. \tag{68}$$

Thus the maximum axial fiber stress can be obtained approximately by multiplying the composite stress by a factor given by a fairly simple formula. For example, with a^2 equal to a quarter (i.e. the fiber diameter is equal to the fiber spacing), the ratio is $(7n+4)/(n+1)$ which, for example, is equal to 6.4 for $n = 4$. It is interesting that the ratio is independent of the aspect ratio of the fiber. This, however, only applies if the fiber is long enough, say with an aspect ratio of 5 or greater.

A further interesting point is that the minimum matrix stress (at $\hat{z} = 0$) is compressive. Expressed as a fraction of the composite stress, the minimum matrix stress $\hat{\sigma}_m^{\min} = \hat{\sigma}_m(0)$ is

$$\frac{\hat{\sigma}_m^{\min}}{\hat{\sigma}_a} = -\frac{n}{n+1}, \tag{69}$$

independent of the volume fraction *and* the fiber aspect ratio (given that the fiber aspect ratio is high enough).

COMPARISON WITH FINITE ELEMENT RESULTS

There are few finite element results available in detail for comparison. The most useful is the analysis by Dragone and Nix (1990), who treated an aluminum alloy with 20% by volume of SiC fibers. A unit cell approach was adopted and calculations performed for $n = 4$. The fiber was perfectly bonded to the matrix and so the relevant comparison is with our results when $\mu = \infty$. A number of features found in the asymptotic analysis are apparent in their steady-state solution for $\alpha = 5$, a somewhat lower aspect ratio than we would prefer for comparison. The stress in the matrix around the fiber is dominated by the hydrostatic stress with the hydrostatic component apparently 25 times the longitudinal deviatoric stress. The hydrostatic stress in the matrix varies almost linearly down the length of the fiber. (Our analysis predicts a variation with $\hat{z}^{1.25}$, but it would be difficult to distinguish this from a linear behavior in numerical results.) The hydrostatic stress adjacent to the fiber is independent of distance from the fiber. The axial stress at the fiber end is about 25% higher than the composite stress indicating an effect of flow around the end of the fiber which we have neglected. The aspect ratio of the cell is equal to the aspect ratio of the fiber. Therefore, by eqn (61), $a^2 = V_f^{2/3}$. For $V_f = 0.2$, this gives $a^2 = 0.34$. For this value of a^2, we predict 4.5 for $\hat{\sigma}_f^{max}/\hat{\sigma}_a$ from eqn (68) and -0.8 for $\hat{\sigma}_m^{min}/\hat{\sigma}_a$ from eqn (69). Dragone and Nix (1990) find these ratios at steady state to be 4.9 and -1.2, respectively. Thus even for the low aspect ratio fiber the asymptotic analysis is reasonably good. We suspect that most of the discrepancy is due to the stress arising from flow around the fiber ends. When the difference between the composite stress and the stress at the fiber end is factored out, our ratios predict the Dragone and Nix (1990) stress values almost exactly. Thus, for longer fibers, we believe our estimates will be quite accurate even without adjustment.

The steady-state strain rates computed by Dragone and Nix (1990) at 80 MPa for fibers with aspect ratios 5, 7 and 10 are listed in Table 1. Also given is a strain rate for an aspect ratio of 20 obtained by extrapolation of the transient results. The matrix steady creep law used by Dragone and Nix (1990) is our eqn (7) with $B = 2 \times 10^{-13}$ when strain rate is given in units of s^{-1} and stress in MPa; as noted before, $n = 4$. The finite element creep strength is computed from eqn (24) and the asymptotic result from eqn (58) with $\mu = \infty$ and $a^2 = V_f^{2/3} = 0.34$ as used in the finite element results. N was taken to be 1 in eqn (58); there is reasonable agreement. The Kelly and Street (1972) predictions for creep strength, based on our eqn (63) with $N = 1$, are also given in Table 1 under the heading "shear lag". They are well below the other results. Dragone and Nix (1990) provide additional results in which the aspect ratio of the cell is varied and the asymptotic solution also agrees reasonably well with those.

Another comparison can be made with the finite element results of Bao *et al.* (1991b). The comparison is made in Table 2. One feature in the results of Bao *et al.* (1991b) is the contrast with the results of Dragone and Nix (1990). Bao *et al.* (1991b) predict lower creep strengths as can be seen in the results for $n = 4$ in Table 2. This suggests that either Dragone and Nix (1990) or Bao *et al.* (1991b) are in error. However, the asymptotic analysis consistently predicts higher strengths than Bao *et al.* (1991b). The substantial differences are probably due to the contribution to the creep strength in the finite element results arising from the fiber end region. The cell length in the finite element calculations is $1/V_f^{1/3}$ times the fiber length. The portion of the cell beyond the fiber ends as a fraction of the whole cell

Table 1. Comparison of steady-state creep results from the finite element calculations of Dragone and Nix (1990) and the asymptotic solution. The results are for 20% SiC fibers in 6061 Al at 80 Mpa. (_____) ≡ extrapolated

Fiber aspect ratio α	Steady creep rate	Creep strength S		
	Finite element results (Dragone and Nix)	Finite elements (Dragone and Nix)	Asymptotic analysis	Shear lag (Kelly and Street)
	s^{-1}			
5	3.5×10^{-8}	3.9	4.5	2.7
7	1×10^{-8}	5.3	6.4	3.6
10	1.5×10^{-9}	8.6	9.4	5.0
20	(7×10^{-11})	(18.5)	21	10.5

Table 2. Comparison of creep strength calculated by Bao *et al.* (1991b) by finite elements with the asymptotic solution. The adjusted column lists $\bar{S} = 1 + V_f^{1/3}(S-1)$ based on the asymptotic solution

Fiber volume fraction V_f	Fiber aspect ratio α	Creep index n	Creep strength S		
			Finite elements (Bao *et al.*)	Asymptotic analysis	Adjusted $\bar{S}$
0.1	5	5	1.8	2.5	1.7
0.1	5	10	1.6	2.2	1.5
0.1	10	5	2.4	4.3	2.5
0.1	10	10	2.1	3.5	2.2
0.2	5	4	3.4	4.5	3.1
0.2	5	5	3.3	4.1	2.8
0.2	5	10	2.9	3.3	2.3
0.2	10	4	4.7	9.4	5.9
0.2	10	5	4.5	8.1	5.2
0.2	10	10	3.9	5.8	3.8

length is $1 - V_f^{1/3}$. This region of the cell experiences relatively unconstrained flow compared to the matrix material surrounding the fiber circumferentially. An estimate of the effect can be made by consideration of radial stressing. The portion of the cell around the fiber would require a radial stress S to produce the same strain rate as unit radial stress would produce in an unconstrained end region. Therefore, the average radial stress on the whole cell for the same strain rate is

$$\bar{S} = 1 + V_f^{1/3}(S-1). \tag{70}$$

This can be converted to an axial stress result by addition of hydrostatic stress. Therefore eqn (70) with S given by the asymptotic solution provides an estimate for the axial creep strength of a unit cell with the same aspect ratio as the fiber. In Table 2 it can be seen that $\bar{S}$ agrees better than S with the creep strength of Bao *et al.* (1991b). There are still discrepancies, but the conversion represented by eqn (70) is an approximation at best. It seems safe to conclude that the asymptotic results should be used for cases where the fiber aspect ratio is greater than 20 so that fiber end effects are less important.

CONCLUSION

An asymptotic solution has been presented for power law creep of a composite material containing aligned, rigid, discontinuous, well bonded high aspect ratio fibers. The solution exhibits several of the features assumed by Kelly and Street (1972) for their shear lag model. These features include the linearity of the axial velocity with distance along the fiber and the dominance of the creep strength by the shearing flow in the matrix. However, asymptotically exact forms for the velocity and stress are provided rather than the estimates used in the shear lag model. The asymptotic solution provides a model for the creep law of the composite material. Although the shear lag creep law of Kelly and Street (1972) exhibits several of the characteristics of the more exact asymptotic creep law, the shear lag model underestimates the creep strength of the composite material. We think this arises from a stress averaging procedure used by Kelly and Street (1972) which seems to be faulty.

The dominant characteristic of the creep law predicted by the asymptotic analysis is that the creep strength is proportional to the fiber aspect ratio raised to the power $1 + 1/n$, where n is the creep exponent. In addition, the model shows that fiber–matrix interface slip can have a disastrous effect on the creep strength of discontinuous fiber composites. If the interface has no shear strength, the creep strength of the composite is approximately equal to the creep strength of the matrix alone. This indicates that such a composite material would creep as fast as the unreinforced matrix at the same applied stress. However, modest levels of interface drag can be mitigated by very long fibers. The effect can be identified in eqn (58) where the interplay between interface drag and aspect ratio is evident. A low drag

coefficient, μ, gives rise to a high value of D. However, very long fibers will have a large aspect ratio leading to high values of λ. The resulting combination can lead to significant creep strengths. Thus continuous fibers, even with occasional breaks, can provide good strengthening even when some interface slip can occur.

The asymptotic solution agrees reasonably well with finite element analyses of the problem. The solution features in the matrix are very similar. Some adjustments have to be made to the creep strength for some of the comparisons to account for the fact that the finite element results were obtained typically for low aspect ratio fibers with unit cells containing substantial volumes of relatively unconstrained matrix beyond the fiber ends. With an appropriate adjustment, there is quite good agreement in terms of the creep strength.

Acknowledgement—This research was supported by the DARPA University Research Initiative at the University of California, Santa Barbara (ONR Contract N00014-86-K0753).

REFERENCES

Bao, G., Genna, F., Hutchinson, J. W. and McMeeking, R. M. (1991a). Models for the strength of ductile matrix composites. In *Intermetallic Matrix Composites*, MRS Symposium Proceedings, Vol. 194 (Edited by D. L. Anton, P. L. Martin, D. B. Miracle and R. M. McMeeking), pp. 3–15. MRS, Pittsburgh.

Bao, G., Hutchinson, J. W. and McMeeking, R. M. (1991b). Particle reinforcement of ductile matrices against plastic flow and creep. *Acta Metall. Mater.* **39,** 1871–1882.

Dragone, T. L. and Nix, W. D. (1990). Geometric factors affecting the internal stress distribution and high temperature creep rate of discontinuous fiber reinforced metals. *Acta Metall. Mater.* **38,** 1941–1953.

Goto, S. and McLean, M. (1991). Role of interfaces in creep of fibre-reinforced metal–matrix composites—II. Short fibres. *Acta Metall. Mater.* **39,** 165–177.

Johnson, R. E. (1984). Power-law creep of a material being compressed between parallel plates: A singular perturbation problem. *J. Engng Math.* **18,** 105–117.

Kelly, A. and Street, K. N. (1972). Creep of discontinuous fibre composites II. Theory for the steady-state. *Proc. R. Soc. Lond.* **A328,** 283–293.

Leckie, F. A. (1986). Micro- and macromechanics of creep rupture. *Engng Fract. Mech.* **25,** 505–521.

Sancaktar, E. and Zhang, P. (1990). Nonlinear viscoelastic modelling of the fiber–matrix interphase in composite materials. *Trans. ASME, J. Mech. Design* **112,** 605–619.

Van Dyke, M. (1975). *Perturbation Methods in Fluid Mechanics*. The Parabolic Press, Stanford, CA.

Weber, C. H., Löfvander, J. P. A., Yang, J. Y., Levi, C. G. and Evans, A. G. (1993). Microstructure and creep of α-TiAl reinforced with Al_2O_3 fibers. *Acta Metall. Mater.* (to appear).

APPENDIX. BOUNDARY LAYER ANALYSIS

According to Johnson (1984), the outer solution velocity equations (54) and (55) prevail into the boundary layer at $z = 0$. Thus in terms of unstretched coordinates with $\eta = z/\delta$ in the boundary layer

$$v_z = \frac{\delta}{D}\left[\frac{1}{\mu 2^n}\left(\frac{1}{a}-a\right)^n + F(r,a,n)\right]\eta \tag{A1}$$

and

$$v_r = -\frac{\delta}{D}\left[\frac{1}{\mu 2^{n+1}}\left(\frac{1}{a}-a\right)^n\left(r-\frac{a^2}{r}\right)+\frac{1}{r}\int_a^r \rho F(\rho,a,n)\,\mathrm{d}\rho\right]. \tag{A2}$$

An effective strain rate can be computed as

$$\varepsilon_e = \sqrt{2/3}\left[\left(\frac{\partial v_r}{\partial r}\right)^2+\left(\frac{v_r}{r}\right)^2+\left(\frac{\partial v_z}{\partial \eta}\right)^2+\frac{1}{2}\left(\frac{\partial v_z}{\partial r}\right)^2\right]^{1/2} \tag{A3}$$

and then the constitutive law provides

$$S_{rr} = \tfrac{2}{3}\varepsilon_e^{(1-n)/n}\frac{\partial v_r}{\partial r}, \tag{A4}$$

$$S_{\theta\theta} = \tfrac{2}{3}\varepsilon_e^{(1-n)/n}\frac{v_r}{r}, \tag{A5}$$

$$S_{zz} = \tfrac{2}{3}\varepsilon_e^{(1-n)/n}\frac{\partial v_z}{\partial \eta}, \tag{A6}$$

and

$$\sigma_{rz} = \tfrac{1}{3}\varepsilon_e^{(1-n)/n}\frac{\partial v_z}{\partial r}. \tag{A7}$$

The hydrostatic stress can be computed from the two equilibrium equations

$$\frac{\partial \sigma}{\partial r} = -\frac{\partial S_{rr}}{\partial r} + \frac{S_{\theta\theta} - S_{rr}}{r} - \frac{\partial \sigma_{rz}}{\partial \eta} \tag{A8}$$

and

$$\frac{\partial \sigma}{\partial \eta} = -\frac{\partial \sigma_{rz}}{\partial r} - \frac{\sigma_{rz}}{r}. \tag{A9}$$

According to Johnson (1984), on the scale of the boundary layer, the hydrostatic stress at leading order is uniform and given by eqn (52) with $z = 0$. It is sustained by tractions on the side of the cell enforcing the constraint that $v_r = -\frac{1}{2}\delta$ there. Therefore, the boundary condition for evaluation of the hydrostatic stress is

$$\sigma(1,0) = -\frac{n^2}{\delta(n+1)(2n+1)D^{1/n}} - S_{rr}(1,0), \tag{A10}$$

which ensures that eqn (23) is satisfied at higher order. At higher order, eqn (23) degenerates to a point wise condition on σ_{rr} because S_{rr} is uniform at $r = 1$ which is a boundary layer also.

Thus by solution of eqns (A8) and (A9) subject to eqn (A10), the stresses can be established throughout the boundary layer at $z = 0$. In particular, σ_{zz} can be computed on $z = 0$. This stress at $z = 0$ plus the axial stress in the fiber at $z = 0$ must be balanced at the other fiber end by an appropriate average stress. The leading order term in eqn (52) at $z = 1$ plus a smaller correction arising from terms computed in eqn (A8) is required. This provides an estimate of the creep strength of the composite material to higher order.

The form of v_z is such that on $z = 0$

$$\frac{\partial \sigma_{rz}}{\partial \eta} = \tfrac{1}{3}\varepsilon_e^{(1-n)/n}\frac{\partial^2 v_z}{\partial r\,\partial \eta} \tag{A11}$$

because, through $(\partial v_r/\partial r)^2$, ε_e depends on η^2. Therefore, on $z = 0$, eqn (A8) becomes

$$\frac{\partial \sigma_{rr}}{\partial r} = \tfrac{2}{3}\varepsilon_e^{(1-n)/n}\left[\frac{v_r}{r^2} - \frac{1}{r}\frac{\partial v_r}{\partial r} - \frac{1}{2}\frac{\partial^2 v_z}{\partial r\,\partial \eta}\right]. \tag{A12}$$

Since $\partial v_z/\partial r = 0$ there, on $z = 0$

$$\varepsilon_e = \sqrt{2/3}\left[\left(\frac{\partial v_r}{\partial r}\right)^2 + \left(\frac{v_r}{r}\right)^2 + \left(\frac{\partial v_z}{\partial \eta}\right)^2\right]^{1/2}, \tag{A13}$$

with v_z and v_r given by eqns (A1) and (A2). To compute the higher order terms in σ_{rr} on $z = 0$, eqn (A12) can be integrated subject to

$$\sigma_{rr}(1,0) = 0, \tag{A14}$$

which is equivalent to eqn (A10) with the leading order term (i.e. the first term on the right-hand side) omitted. The result for $\sigma_{rr}(r,0)$ can be used to compute the axial stress from

$$\sigma_{zz}(r,0) = \sigma_{rr}(r,0) + S_{zz}(r,0) - S_{rr}(r,0). \tag{A15}$$

The net resultant in the boundary layer is

$$2\pi\int_a^1 \sigma_{zz}(r,0) r\,\mathrm{d}r = \delta^{1/n} N\pi, \tag{A16}$$

which defines N. Two cases can be considered. One situation arises if μ is large or infinite and there is little or no slip at the fiber–matrix interface. This is the high drag case. In that situation N only becomes important in the creep strength at small volume fractions of fibers. The other case is where μ is small or zero so that the matrix is free or almost free to slip against the fiber without drag.

High drag interface

In this case, D in eqn (51) is large only if a is small. With D large, the leading order stress estimate at $z = 1$ can be modest in magnitude and the higher order corrections are significant. Investigation of the velocities in eqns (A1) and (A2) reveals that when a is small, the term containing μ can be neglected and the effective strain rate ε_e on $z = 0$ is almost uniform except when r is just slightly larger than a. However, the strain rates tend rapidly to

zero at $r = a$ and according to eqns (A4)–(A6) so do the deviatoric stresses. Consequently, the small region around the fiber with r slightly larger than a will contribute very little to the stress resultant N. In view of this, a treatment will be reasonably accurate with ε_e taken to be uniform everywhere on $z = 0$ but with the strain rate components allowed to vary otherwise according to eqns (A1) and (A2).

With the strain rates computed from eqns (A1) and (A2) (with $\mu \to \infty$) eqn (A12) becomes

$$\frac{\partial \sigma_{rr}}{\partial r} = -\tfrac{2}{3}\varepsilon_e^{(1-n)/n}\frac{\delta}{D}\left[\frac{2}{r^3}\int_a^r \rho F(\rho, a, n)\,d\rho - \frac{1}{r}F(r, a, n) + \frac{1}{2}\frac{\partial F(r, a, n)}{\partial r}\right]. \tag{A17}$$

With ε_e uniform, this integrates, subject to eqn (A14) to give

$$\sigma_{rr} = \tfrac{2}{3}\varepsilon_e^{(1-n)/n}\frac{\delta}{D}\left[\frac{1}{r^2}\int_a^r \rho F(\rho, a, n)\,d\rho - G(a, n) - \tfrac{1}{2}F(r, a, n) + \tfrac{1}{2}F(1, a, n)\right]. \tag{A18}$$

On $z = 0$, from eqns (A4) and (A6)

$$S_{zz} - S_{rr} = \tfrac{2}{3}\varepsilon_e^{(1-n)/n}\frac{\delta}{D}\left[2F(r, a, n) - \frac{1}{r^2}\int_a^r \rho F(\rho, a, n)\,d\rho\right] \tag{A19}$$

so

$$\sigma_{zz} = \tfrac{2}{3}\varepsilon_e^{(1-n)/n}\frac{\delta}{D}[\tfrac{3}{2}F(r, a, n) + \tfrac{1}{2}F(1, a, n) - G(a, n)] \tag{A20}$$

which is valid for r close to 1 but suspect for r close to a. Calculation of N from eqn (A18) then gives

$$N = \delta^{-1/n}\varepsilon_e^{(1-n)/n}\frac{\delta}{D}[\tfrac{2}{3}(2 + a^2)G(a, n) + \tfrac{1}{3}(1 - a^2)F(1, a, n)]. \tag{A21}$$

This result is most readily utilized for even integer positive values of n. In that case, calculation of $F(1, a, n)$ and $G(a, n)$ can be carried out by binomial expansion. In addition, the leading terms in ε_e can be computed at $r = 1$. The result to leading terms is

$$N = 1 - \frac{(2n^2 - 2n - 7)(n - 1)}{6n(n - 3)}a^2 + \cdots. \tag{A22}$$

Low drag interface

In this situation, μ is close to zero. The limiting case of $\mu \to 0$ (no drag) will be considered. As a consequence, the velocities in eqns (A1) and (A2) become

$$v_z = \frac{\eta\delta}{1 - a^2} \tag{A23}$$

and

$$v_r = -\frac{\delta}{1 - a^2}\frac{1}{2}\left(r - \frac{a^2}{r}\right) \tag{A24}$$

and $D = \infty$. This is a planar flow in the fiber direction, as would be expected when there is no drag. The effective strain rate is

$$\varepsilon_e = \frac{\delta}{1 - a^2}\left[1 + \frac{1}{3}\frac{a^4}{r^4}\right]^{1/2} \tag{A25}$$

and integration of eqn (A12) gives, on $z = 0$,

$$\sigma_{rr} = -\frac{2}{3}\left(\frac{\delta}{1 - a^2}\right)^{1/n}\int_r^1 \left[1 + \frac{1}{3}\frac{a^4}{r^4}\right]^{(1-n)/2n}\frac{a^2}{r^3}\,dr. \tag{A26}$$

The deviatoric stresses are such that

$$S_{zz} - S_{rr} = \frac{2}{3}\left(\frac{\delta}{1 - a^2}\right)^{1/n}\left[1 + \frac{1}{3}\frac{a^4}{r^4}\right]^{(1-n)/2n}\left[\frac{3}{2} + \frac{1}{2}\frac{a^2}{r^2}\right]. \tag{A27}$$

Finally, the stress σ_{zz}, the sum of eqns (A26) and (A27), can be integrated to give

$$N = \frac{4/3}{(1 - a^2)^{1/n}}\int_a^1 \left[1 + \frac{1}{3}\frac{a^4}{r^4}\right]^{(1-n)/2n}\left[\frac{3}{2}r + \frac{a^4}{2r^3}\right]dr. \tag{A28}$$

Note that when $a = 0$, $N = 1$, as in eqn (A22).